Title

Targeted Proteomics of the Eicosanoid Biosynthetic Pathway Completes an Integrated Genomics-Proteomics-Metabolomics Picture of Cellular Metabolism*

Journal

Molecular & Cellular Proteomics, 11(7)

ISSN

1535-9476

Authors

Sabidó, Eduard
Quehenberger, Oswald
Shen, Qin
et al.

Publication Date

2012-07-01

DOI

10.1074/mcp.m111.014746

Peer reviewed

Targeted Proteomics of the Eicosanoid Biosynthetic Pathway Completes an Integrated Genomics-Proteomics-Metabolomics Picture of Cellular Metabolism*[S]

Eduard Sabidó‡§, Oswald Quehenberger¶, Qin Shen‡, Ching-Yun Chang‖, Ishita Shah, Aaron M. Armando**, Alexander Andreyev**, Olga Vitek‖, Edward A. Dennis**‡‡, and Ruedi Aebersold‡§ §§¶¶**

Eicosanoids constitute a diverse class of bioactive lipid mediators that are produced from arachidonic acid and play critical roles in cell signaling and inflammatory aspects of numerous diseases. We have previously quantified eicosanoid metabolite production in RAW264.7 macrophage cells in response to Toll-like receptor 4 signaling and analyzed the levels of transcripts coding for the enzymes involved in the eicosanoid metabolite biosynthetic pathways. We now report the quantification of changes in protein levels under similar experimental conditions in RAW264.7 macrophages by multiple reaction monitoring mass spectrometry, an accurate targeted protein quantification method. The data complete the first fully integrated genomic, proteomic, and metabolomic analysis of the eicosanoid biochemical pathway. ***Molecular & Cellular Proteomics 11: 10.1074/mcp.M111.014746, 1–9, 2012.***

Eicosanoids constitute a diverse class of bioactive lipid mediators produced from arachidonic acid that play critical roles in cell signaling and inflammatory aspects of numerous diseases (1–3). Under basal conditions, biological systems have very low levels of free fatty acids including arachidonic acid, because fatty acids are mostly found esterified in triglycerides, sterol esters, and phospholipids. The activation of specific receptors causes many downstream events, including triggering the release of free arachidonic acid from membrane phospholipids by the action of phospholipase A_2 and its subsequent conversion to oxygenated metabolites generally termed eicosanoids (4). We have previously quantified eicosanoid metabolite production in RAW264.7 macrophage cells (5, 6) in response to the Toll-like receptor 4 (TLR-4)[1] agonist Kdo_2-lipid A (KLA), a single well defined subspecies of lipopolysaccharide and a potent inducer of macrophage inflammatory programs (7). We also carried out a fluxomic analysis of the metabolic profile as a function of time after stimulation (8) and a transcriptomic analysis as part of a broader study of the macrophage lipidome and its transcriptomic correlation (9). We now report the quantification of changes in abundances of the proteins involved in eicosanoid biosynthesis under similar experimental conditions, using multiple reaction monitoring, a quantitatively accurate targeted mass spectrometric method. The results complete the first fully integrated genomic, proteomic, and metabolomic analysis of the eicosanoid biochemical pathway using mouse RAW264.7 cells as a model system.

EXPERIMENTAL PROCEDURES

Sample Preparation—RAW 264.7 macrophages (American Type Culture Collection, catalog number TIB-71) were seeded at a density of 1×10^7 cells into 75-cm^2 tissue culture flasks and grown for 18 h to reach a density of $\sim 2 \times 10^7$ cells/flask in DMEM (without phenol red) supplemented with 4 mM L-glutamate, 4.5 g $liter^{-1}$ D-glucose, 10% heat-inactivated FCS, and 1% penicillin/streptomycin (Invitrogen). The cells were stimulated with KLA (100 ng ml^{-1} final concentration) and harvested at 0.5, 1, 2, 4, 8, 12, and 24 h after stimulation. Control cells were collected at 0 and 24 h after the addition of Dulbecco's PBS. In the case of double-stimuli time courses, the cells were treated with KLA (100 ng ml^{-1}), and after 4 h, the macrophages were stimulated with ATP (final concentration, 2 mM). The cells were harvested at 0, 2, 4, 8, and 20 h after the treatment with ATP; nonstimulated control cells were collected at 0 and 24 h after the addition of Dulbecco's PBS. All of the experiments were done in triplicate.

The cell pellets were homogenized using radioimmune precipitation assay-modified buffer (1% Nonidet P-40, 0.1% sodium deoxycholate, 150 mM NaCl, 1 mM EDTA, 50 mM Tris, pH 7.5, protease inhibitors EDTA-free, 10 mM NaF, 10 mM sodium pyrophosphate, 5

From the ‡Department of Biology, Institute of Molecular Systems Biology and the §Competence Center for Systems Physiology and Metabolic Disease, ETH Zurich, 8093 Zurich, Switzerland, the ¶Departments of Medicine and of Pharmacology and the **Departments of Chemistry and Biochemistry and of Pharmacology, School of Medicine, University of California, San Diego, La Jolla, CA, 92093-0601, the ‖Departments of Statistics and Computer Science, Purdue University, West Lafayette, Indiana 47107, and the §§Faculty of Science, University of Zurich, 8057 Zurich, Switzerland

Received October 4, 2011, and in revised form, January 8, 2012
Published, MCP Papers in Press, February 23, 2012, DOI 10.1074/mcp.M111.014746

[1] The abbreviations used are: TLR, Toll-like receptor; KLA, Kdo_2-lipid A; MRM, multiple reaction monitoring.

mM 2-glycerophosphate) and a glass-glass tight Dounce homogenizer (Wheaton Science Products). The homogenates were centrifuged (20,000 × *g* at 4 °C for 15 min), and the supernatant was collected and kept at 4 °C. The pellets were resuspended with urea-Tris buffer (50 mM Tris, pH 8.1, 75 mM NaCl, 8 M urea, EDTA-free protease inhibitors, 10 mM NaF, 10 mM sodium pyrophosphate, 5 mM 2-glycerophosphate). After sonication, the samples were centrifuged again (20,000 × *g* at 4 °C for 15 min). The resulting supernatant was collected and mixed with the previous supernatant. The resulting pellets were discarded. The total protein content was quantified with the BCA Protein Assay (Thermo Fisher Scientific) using bovine serum albumin as standard. Aliquots of the homogenates were immediately prepared and stored at −80 °C. The sample quality and concentration was double checked with SDS-PAGE and silver staining (supplemental Fig. S1).

A 100-μg aliquot of total protein was mixed with 100 μg of the heavy isotope-labeled reference proteome (see below), and the combined sample was precipitated overnight with 6 volumes of ice-cold acetone (16 h, −20 °C) for mass spectrometric analysis. The supernatant was discarded, and the pellets were dried and resuspended in freshly prepared digestion buffer (8 M urea, 0.1 M NH_4HCO_3). The samples were reduced with 12 mM dithiothreitol (30 min, 37 °C) and alkylated with 40 mM iodoacetamide (45 min, 25 °C) in the dark. The samples were diluted with 0.1 M NH_4HCO_3 to a final concentration of 1.5 M urea and digested overnight at 37 °C with sequence grade trypsin (1 μg; Promega AG). After digestion, the peptide mixtures were acidified to pH 2.8 with trifluoroacetic acid and desalted with MacroSpin C_{18} silica columns (The Nest Group Inc.). The samples were dried under vacuum and resolubilized to 1 μg μl^{-1} in 0.1% formic acid and 2% acetonitrile prior to mass spectrometric analysis.

Preparation of the Heavy Isotope-labeled Reference Proteome—A Hepa1–6 mouse cell line was obtained from the American Type Culture Collection (catalog number CRL-1830), labeled with stable isotope labeling of amino acids in cell culture medium and used as a heavy labeled reference proteome in all samples. The cells were grown at 37 °C and 5% CO_2 in L-lysine- and L-arginine-depleted high glucose DMEM (Caisson Laboratories Inc.) supplemented with 10% dialyzed FCS (BioConcept), 1% penicillin/streptomycin (Invitrogen), and L-$^{13}C_6{}^{15}N_4$-arginine and L-$^{13}C_6{}^{15}N_2$-lysine (Sigma-Aldrich). The cells were cultured in 150-cm^2 plates (Nunclon) and passaged at 80% confluence. The incorporation of the heavy amino acids was regularly checked by mass spectrometry on cell aliquots, and the culture was maintained until an incorporation of >95% was achieved. The cells were then washed with ice-cold PBS, scraped from the plates, and homogenized as described above.

Multiple Reaction Monitoring Assay Development—Multiple reaction monitoring (MRM) assays were developed following the general high throughput strategy previously reported (10). Initially, four to six unique peptides ranging from 6 to 20 amino acids in length containing tryptic ends and no miscleavages were chosen for each of the selected proteins. Unique peptides previously observed in MS experiments (11, 12) were prioritized during the peptide selection process. For those proteins for which no peptides had been reported previously (previously unidentified proteins), peptide selection was based on the MS suitability score computed by PeptideSieve (13). All of the peptides containing amino acids prone to undergo nonspecific reactions (Met, Trp, Asn, and Gln) were avoided and only selected when no other options were available (14). The selected peptides were chemically synthesized via SPOT synthesis (JPT Peptide Technologies) and used in unpurified form for the MRM assay development. Fragment ion spectra were collected in MRM-triggered MS^2 mode for each peptide in a QTRAP 4000 instrument (AB/SCIEX). The spectra were used to confirm identities, to extract the optimal fragment ions for MRM analysis, and to obtain peptide retention times. MS^2 data were analyzed with the Mascot search engine (v. 2.1; MatrixScience) against a customized mouse Uniprot database (dated July 2009) containing all of the selected proteins and the corresponding decoy entries generated by reversing the amino acid sequences of the tryptic peptides. Search parameters were set to 2.0 Da for the precursor mass tolerance, 0.8 Da for the fragment mass tolerance, fully tryptic peptides, no miscleavages, and a false discovery rate of 1% based on decoy assignments (15). Cysteine carbamidomethylation was set as a fixed modification, and methionine oxidation was used as a variable modification. A spectral library was generated from the validated fragment ion spectra using in-house-written Perl scripts, and for each spectrum, the four most intense y ions were selected as optimal MRM transitions to be monitored. Mass spectrometry parameters, such as collision energy and declustering potential, and further details on the generation of the peptide library, development of MRM assays, and spectral library creation can be found in previous reports (10, 16).

Measurements and Data Analysis—MRM measurements were performed on a hybrid triple quadrupole/ion trap mass spectrometer (4000 Q-Trap; AB/Sciex) equipped with a nano-LC electrospray ionization source. Fused silica microcapillary columns (75 μm) were pulled and packed with Magic C_{18} AQ 5-μm reverse phase material (Michrom BioResources). Samples (2 μg) were loaded onto a 2.5-cm precolumn (100 μm; New Objective) packed with C_{18} reverse phase material and were analyzed with a linear gradient from 5 to 30% of buffer B in 30 min at a flow rate of 300 nl min^{-1} using a Tempo nanoLC system (Applied Biosystems). Buffer A contained 98% H_2O, 2% ACN, and 0.1% formic acid; Buffer B contained 2% H_2O, 98% ACN, and 0.1% formic acid. Blank runs were performed between the MRM measurements of biological samples to avoid sample carryover. Measurements were done in scheduled MRM mode, using a retention time window of 5 min, ~400 transitions per method, and a cycle time of 2.5 s. These parameters ensured a dwell time of over 10 ms/transition. Three replicates for each time point were used in these measurements.

Transition groups corresponding to the targeted peptides were evaluated with MultiQuant v. 1.1 Beta (Applied Biosystems) based on (i) coelution of the transition traces associated with a targeted peptide, both in its light and heavy forms; (ii) presence of at least four coeluting transition traces for a given peptide exceeding a signal-to-noise ratio of 3; (iii) correlation between the light MRM relative intensities and the heavy counterparts; (iv) correlation between the MRM relative intensities and the intensities obtained in the MS^2 spectra during the MRM assay development; and (v) consistency among replicates.

Initially all peak intensities were transformed by the logarithm based 2, and transitions with completely missing intensities in more than two-thirds of the stage conditions were removed. A constant normalization was performed to all measurements to equalize the median peak intensities of reference transitions between runs (17). The remaining normalized MRM peak intensities were retained for quantitative analysis. In summary, a set of 29 target proteins were represented by one to four peptides each, and each peptide was represented by two to four pairs of light-heavy transitions. Protein level quantification and testing for differential abundance were performed using a linear mixed effects model (18), as outlined in the MSstats software package (http://www.stat.purdue.edu/~ovitek/Software.html). A list of *p* values was calculated separately for each comparison and was adjusted to control the false discovery rate at the cutoff 0.01 (19).

Statistical Analyses—The Spearman's rank correlation, which is a nonparametric method to measure a statistical dependence between two variables, was used to test the statistical correlation between

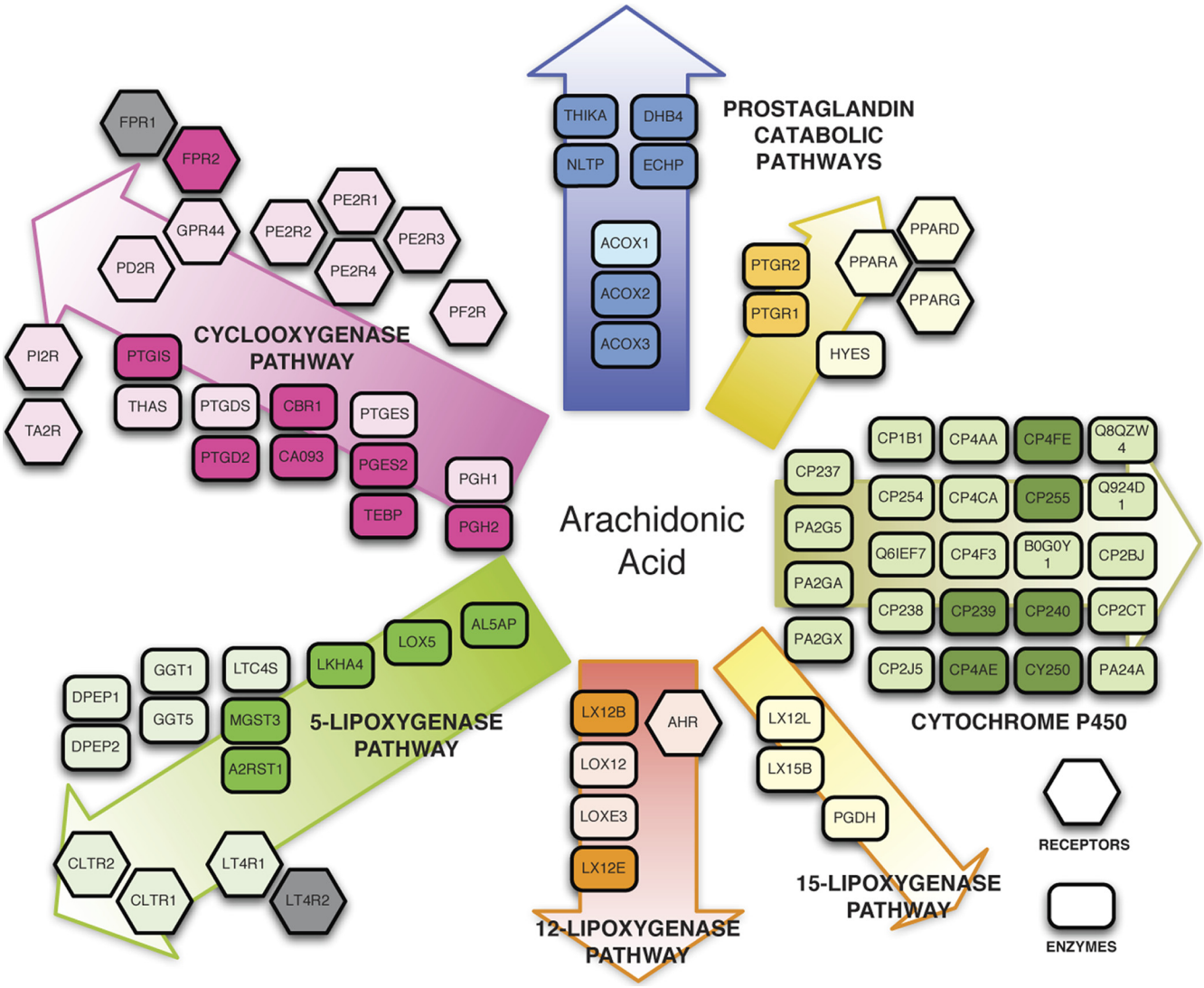

FIG. 1. **Schematic representation of the proteins involved in the different pathways related to eicosanoid biosynthesis.** Highlighted in *color* are proteins for which MRM assays have been developed, and among them, dark-colored proteins have been detected and quantified in RAW264.7 murine macrophage whole cell extracts by MRM targeted proteomics. Those proteins for which no MRM assays could be developed are in *dark gray*.

transcriptomic and proteomic data sets. Transcriptomics and proteomics fold changes (Ti, Pi) for each transcript and corresponding protein of time course experiments were converted to ranks (ti, pi), and the Spearman's rank correlation coefficient (ρ) was calculated from the ranked fold changes as the Pearson correlation coefficient between the variables Ti and Pi. In general, numeric values range from $+1$ to -1, with $\rho > 0$ indicating a positive correlation, with $\rho < 0$ indicating a correlation in the opposite direction and $\rho = 0$ indicating no correlation.

RESULTS

MRM assays were initially designed to map the complete set of proteins involved in the eicosanoid biosynthesis pathway (4) (Fig. 1 and supplemental Table 1). MRM assays corresponding to two to four unique peptides/protein were developed with synthetic peptides following the general high throughput strategy previously reported (10). Unique peptides were selected based on the number of observations in previous MS experiments (11, 12) or, when no previous evidence was available, on the MS suitability score predicted by PeptideSieve (13). From these peptides, we generated a spectral library containing MRM assays for 79 eicosanoid-related proteins (supplemental Table 1) that is presented here as an easy and convenient tool for the eicosanoid research community to target and rapidly quantify multiple proteins under different conditions and treatments. To further illustrate the utility of the developed MRM assays, we used them to study the effect of KLA and ATP on the eicosanoid-related proteome and to integrate these results with our previously acquired transcriptomic and fluxomic data, thus completing the first fully integrated genomic, proteomic, and metabolomic analysis of the eicosanoid biochemical pathway.

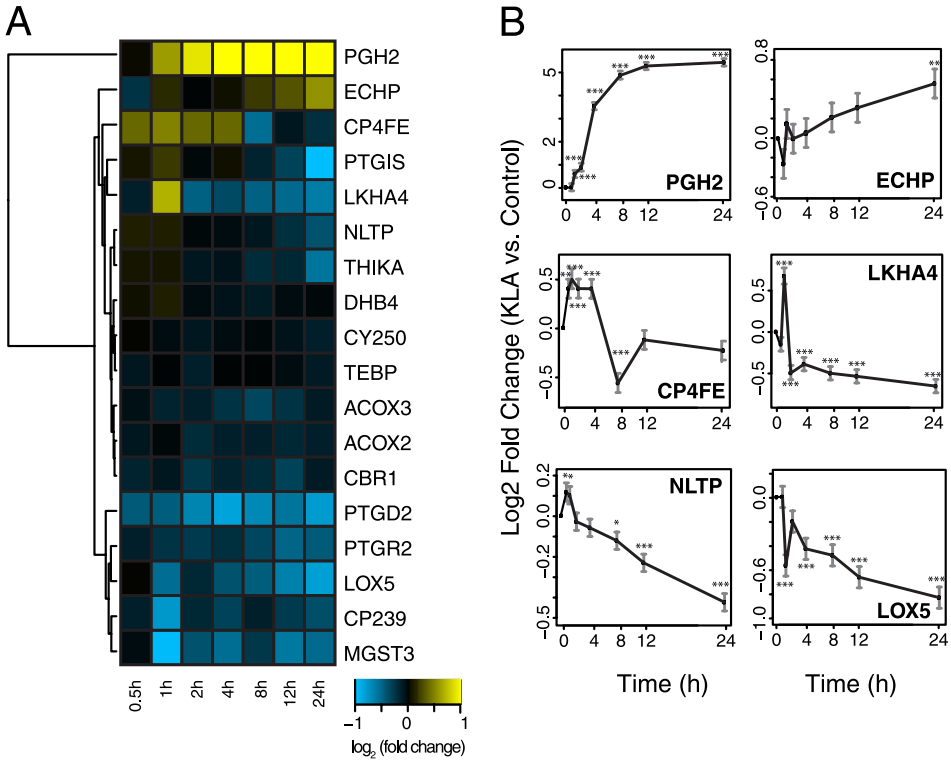

FIG. 2. *A*, changes in protein abundance at 0.5, 1, 2, 4, 8, 12, and 24 h after macrophage stimulation with KLA. Only proteins with a significant fold change in at least one time point are presented. All of the time points were compared with an untreated control sample (without KLA). The colors represent either increased (*yellow*) or decreased (*blue*) protein abundances, whereas the intensity reflects the corresponding $\log_2$(fold change). *B*, logarithmic fold change profiles of selected proteins after KLA treatment of macrophages. The *error bars* represent the standard error of the mean. ***, p value < 0.001; **, $0.001 < p$ value < 0.01; *, $0.01 < p$ value < 0.05. All of the experiments were done in triplicate. The protein codes refer to the Uniprot database identifiers without the suffix _MOUSE.

Cells were initially challenged with KLA (7) to induce an inflammatory response and harvested at 0, 0.5, 2, 4, 8, 12, and 24 h after the treatment. Cells lacking KLA treatment at 0 and 24 h were used as controls. The cell extracts were analyzed by MRM without further fractionation, and detected peptides were quantified based on peak height and compared with those of untreated control samples (supplemental Table 2). A total of 29 proteins involved in all branches of the eicosanoid biosynthetic pathway (Fig. 1) (4) could be detected and quantified in unfractionated RAW264.7 murine macrophage cell extracts by MRM targeted proteomics (supplemental Table 3).

MRM measurement reproducibility was checked through comparison of the normalized peak intensities across the three biological replicates (supplemental Figs. S2 and S3). Several changes in the protein abundance profiles were observed, and up to 18 of the 19 monitored proteins showed significant changes in protein abundance in response to KLA treatment, including cyclooxygenase-2 and leukotriene A-4 hydrolase, both of which play key roles in the synthesis of prostaglandins and leukotrienes (Fig. 2 and supplemental Fig. S4 and Table 2).

Protein abundance profiles were then compared with the transcriptomic data that we had previously acquired under identical experimental conditions (9). For each protein and transcript pair, a nonparametric Spearman's rank correlation coefficient (ρ) was calculated to estimate their statistical dependence (supplemental Table 4). Although many proteins showed either a positive correlation between protein and transcript abundance or a negative correlation in the opposite direction (Fig. 3 and supplemental Fig. S5), others showed no correlation (*e.g.* peroxisomal acyl-coenzyme A oxidase 2). It is therefore clear that the discordant protein profiles could not have been predicted from the transcript levels, which highlights the importance of measuring protein abundances and generating a proteomic data set to complement the available transcriptomic and lipidomic data sets to better understand the system under study.

To further examine the dynamics of the eicosanoid biosynthetic system, we performed additional MRM measurements to quantify the eicosanoid-related proteome response to a combined KLA and ATP stimulation of macrophages, designed to serve as a priming experiment for a purinergic receptor (6). To determine whether ATP could enhance the inflammatory response beyond the effects of KLA, we first primed macrophage cells with KLA and then performed a second stimulation with ATP after 4 h. The cells were harvested at 0, 2, 4, 8, and 20 h after ATP stimulation, and cells

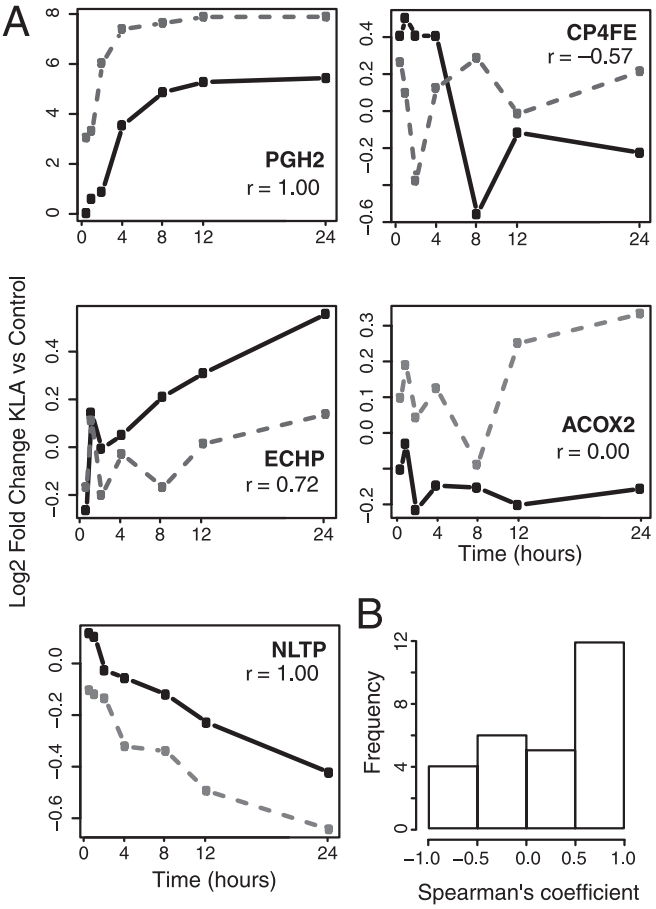

FIG. 3. *A*, profile plots of protein (*solid black lines*) and transcript (*dotted gray lines*) fold changes upon KLA cell stimulation with their corresponding Spearman's rank correlation coefficient (ρ). *B*, distribution of Spearman's rank correlation coefficients calculated for all detected protein-transcript pairs.

not subjected to the stimuli were used as controls. The results were compared with the corresponding fold changes obtained from the KLA-only treatment of the macrophages (Fig. 4).

The KLA/ATP double stimulation produced significant changes in the abundance of 19 proteins when compared with nonstimulated controls (Fig. 4*A*). Although many of these changes were similar to those observed in the KLA-treated macrophages, some significant differences were noted when comparing the results of the KLA-only and KLA/ATP treatments. First, the KLA/ATP stimulation showed a stronger effect on the activation of prostaglandin biosynthesis, producing higher levels of cyclooxygenase-2 (or prostaglandin G/H synthase 2, PGH2) than KLA-only stimulation. Second, the combined stimulation protocol produced an increase in PGH2 levels that was sustained even at later time points (Fig. 4*C*). Third, other enzymes in this pathway, including prostaglandin D synthase (PTGD2) that did not significantly change with KLA treatment alone, now showed a significant increase in protein abundance. Other enzymes of the eicosanoid biosynthetic system, such as microsomal glutathione *S*-transferase 3 (MGST3), leukotriene A-4 hydrolase, and 12-lipoxygenase, showed either no significant change or a slight decrease in protein abundance when compared with the KLA-only treatment.

DISCUSSION

In the present work, we present the development of a set of MRM assays for 79 eicosanoid-related proteins as an easy and convenient tool for the eicosanoid research community to rapidly quantify multiple proteins under different conditions and treatments. We illustrate the utility of these assays by studying the effect of KLA and ATP on the eicosanoid-related proteome in RAW 264.7 macrophages, and we integrate these results with our previously acquired transcriptomic and metabolite fluxomic data.

KLA treatment of the murine macrophage cells reveals several significant changes in protein abundance (Fig. 2 and supplemental Fig. S4 and Table 2). Among the proteins that showed significant changes in abundance over time, cyclooxygenase-2 (PGH2) showed an early increase in protein abundance in excess of 32-fold over the basal level after 8 h of treatment. Thereafter, the protein level remained constant even 24 h after stimulation. Cyclooxygenase-2 is an important component of the inflammatory response of macrophages because it catalyzes the rate-limiting step of prostaglandin biosynthesis. The strong increase in the observed level of cyclooxygenase-2 in stimulated macrophages not only agrees with our previously obtained transcriptomic data (Fig. 3) (9), but it is also consistent with the increased formation of prostaglandins, including prostaglandins D2, E2, F2α, and J2, reported in our previous studies (supplemental Table 6). These results confirm the importance of protein cyclooxygenase-2 in the macrophage inflammatory response to KLA (20, 21). Other proteins involved in the pathway showed either no significant change in protein abundance—such as prostaglandin 9-ketoreductase (CBR1), prostaglandin F synthase (CA093), and prostaglandin E synthase 2—or a slight decrease that showed a good correlation with transcriptomics data (Fig. 5). Even though the expression levels of various terminal synthases remain unchanged in activated cells, KLA as well as ATP robustly stimulated prostaglandin formation. These observations suggest that in addition to transcription, other regulatory mechanisms are utilized for optimal cellular eicosanoid synthesis in response to pro-inflammatory stimuli.

In addition to changes in gene expression and protein abundance, enzyme activity can also be regulated by mechanisms involving post-translational modifications and/or protein translocation. The liberation of free arachidonic acid or related polyunsaturated acids by members of the phospholipase A_2 superfamily, most prominently by Group IV cPLA$_2$, is the key initiating step of the various eicosanoid biosynthetic pathways (22). The activity of Group IV cPLA$_2$ is regulated by intracellular calcium and the binding of calcium to specific

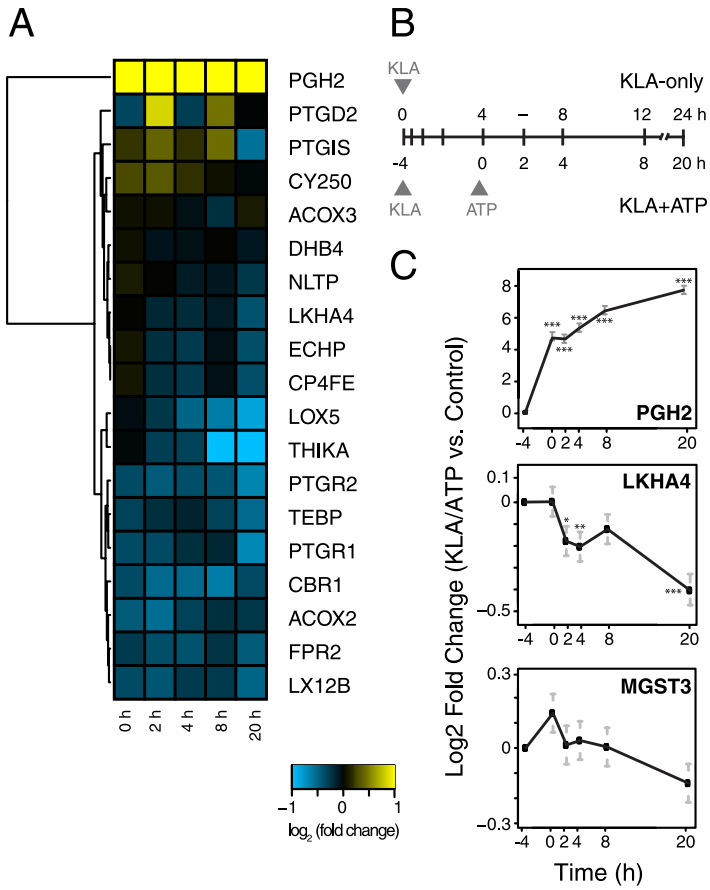

FIG. 4. *A*, changes in protein abundance at 0, 2, 4, 8, and 20 h after macrophage stimulation with KLA + ATP. The cells were pretreated for 4 h with KLA before the addition of ATP. The time course refers to ATP treatment. Only proteins with a significant fold change in at least one time point are represented. All time points were compared with an untreated control sample (without KLA or ATP). The colors represent either increased (*yellow*) or decreased (*blue*) protein abundances, whereas intensity reflects the corresponding $\log_2$(fold change). *B*, time scale comparison between the KLA-only and the KLA + ATP experiments. *C*, logarithmic fold change profiles of selected proteins after KLA + ATP treatment of macrophages, compared with untreated control cells (without KLA or ATP). The *error bars* represent the standard error of the mean. ***, p value < 0.001; **, $0.001 < p$ value < 0.01; *, $0.01 < p$ value < 0.05. All of the experiments were done in triplicate. The protein codes refer to the Uniprot database identifiers without the suffix _MOUSE.

protein domains induces a translocation of the enzyme to membranes, where phospholipids serve as substrates. The enzyme is activated very rapidly within minutes by agonists that induce intracellular calcium fluxes via mechanisms that do not involve protein synthesis. The stimulation of the TLR-4 pathway by KLA does not induce measurable changes in intracellular calcium; nevertheless, it causes a robust increase in free arachidonate, albeit at a slower rate compared with calcium agonists. In the absence of calcium signals, the obligatory translocation and activation of Group IV $cPLA_2$ may occur via mechanisms that involve ceramide-1 phosphate or phosphatidylinositol 4,5-bisphosphate (22). The production of prostaglandins is further controlled by the activities of cyclooxygenase enzymes. Cyclooxygenase-1 is constitutively expressed, whereas cyclooxygenase-2 is strongly induced by KLA or by the combination of KLA and ATP (Figs. 1 and 4). The resulting metabolite of cyclooxygenase activation, PGH2, serves as a substrate for the terminal synthases of prostaglandin production (Fig. 5). In contrast to the activity of cyclooxygenase-2, which is primarily controlled by expression, the activity of 5-lipoxygenase in leukotriene biosynthesis is regulated at the post-transcriptional level (23). The availability of free arachidonic acid is a major determinant of leukotriene biosynthesis. In fact, stimuli effective in inducing leukotriene formation, *e.g.*, inflammatory agents that cause release of intracellular calcium, cause robust activation of both Group IV $cPLA_2$ and 5-lipoxygenase (24). Furthermore, both Group IV $cPLA_2$ and 5-lipoxygenase share similar structural, regulatory, and phosphorylation domains, and upon cell stimulation, both enzymes translocate to the nuclear membrane, where the conversion of arachidonic acid to leukotrienes is thought to occur (25). Membrane-bound helper protein 5-lipoxygenase activating protein facilitates the transfer of free arachidonic acid to 5-lipoxygenase and is essential for efficient enzyme utilization.

Although activation of the TLR-4 pathway by itself does not trigger leukotriene synthesis, this pathway is well known to prime cells for enhanced leukotriene formation in response to triggering stimuli. Consistent with this concept, several members of the 5-lipoxygenase pathway showed significant changes upon KLA stimulation of RAW264.7 cells. Incidentally, leukotriene A-4 hydrolase, which catalyzes the final step in the biosynthesis of the proinflammatory mediator leukotriene B4, showed a significant reduction at the protein level, particularly after several hours of KLA treatment (Fig. 2 and supplemental Fig. S4). This finding is consistent with the previous observations that challenge of RAW264.7 cells with TLR-4 agonists leads to the production of prostaglandins but does not induce the formation of leukotrienes, which critically depends on intracellular calcium fluxes (6). However, even

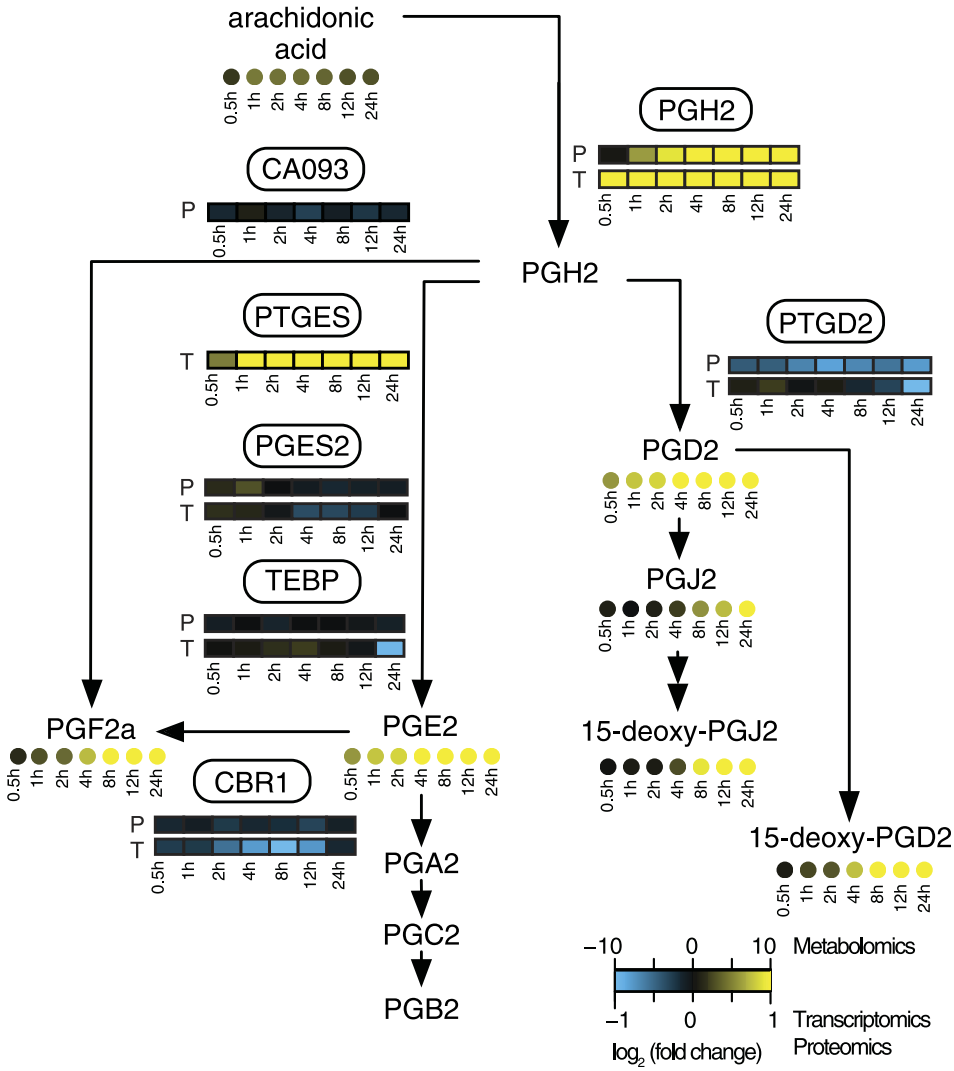

FIG. 5. **Schematic overview of transcriptomics, proteomics and metabolomics changes in the prostaglandin biosynthetic pathway at 0.5, 1, 2, 4, 8, 12, and 24 h after macrophage stimulation with KLA.** Transcriptomics (*T*), proteomics (*P*), and metabolomics (*circles*) data are represented as individual heat maps for each transcript, protein, and metabolite, in which colors represent either increased (*yellow*) or decreased (*blue*) abundance, with the intensity reflecting the corresponding $\log_2$(fold change). All of the time points were compared with an untreated control sample (without KLA). Only transcriptomic data were obtained for microsomal prostaglandin E synthase 1 PTGES.

though KLA by itself does not stimulate the 5-lipoxygenase pathway in macrophages, several studies showed that it potently primes macrophages for enhanced leukotriene release in response to calcium agonists (6, 26, 27). This priming effect appears to be maximal at the early stages of the KLA challenge but dissipates after prolonged exposure. Consistent with these observations, we find an initial but transient increase in the leukotriene A-4 hydrolase protein (Fig. 2 and supplemental Fig. S4), which may in part explain the time restrictions on the KLA priming effect. In addition, prolonged exposure to TLR-4 agonists induces nitric oxide synthesis, which has been shown to inhibit the 5-lipoxygenase pathway (24, 25). Accordingly, other members of the leukotriene biosynthetic pathway, such as 5-lipoxygenase and microsomal glutathione *S*-transferase 3, also showed significant decreases in protein levels at the later stages of KLA treatment. A positive response was observed in the cytochrome leukotriene-B4 omega-hydroxylase 3 (CP4FE), an enzyme presumably involved in the inactivation of leukotriene B4 by hydroxylation (26).

In addition to the enzymes related to prostaglandin and leukotriene biosynthesis, a general decrease in abundance of many enzymes involved in the catabolism of prostaglandins was observed. This was the case for acetyl-CoA oxidase 2 and 3, prostaglandin reductase 2, peroxisomal 3-oxoacyl-CoA thiolase A, and the propanoyl-CoA C-acyltransferase, all of which showed a consistent decrease at the protein level over time (Fig. 2 and supplemental Fig. S4). Only the protein 3-hydroxyacyl-

CoA dehydrogenase (ECHP) showed a significant increase at the later time points of KLA stimulation. No significant changes were observed for proteins related to the 12-lipoxygenase and 15-lipooxygenase pathways, which is in agreement with the previously reported transcriptomic data and suggests that KLA treatment has no effect on these pathways.

The dynamics of the eicosanoid biosynthetic system was further studied with a combined KLA and ATP stimulation of macrophages. ATP is known to be released after the adjuvant stimulation of Toll-like receptors. The released ATP interacts with the ATP-gated calcium channel P2X4 triggering a calcium influx that initiates the inflammatory response (28). Indeed, the combined KLA and ATP stimulation of macrophages was designed to serve as a priming experiment for a purinergic receptor (6).

The additional MRM measurements to quantify the eicosanoid-related proteome response to a KLA/ATP double treatment revealed significant changes in the abundance of several proteins when compared with both nonstimulated controls and KLA-only treatment (Fig. 4*A* and supplemental Table 7). As outlined above, KLA/ATP stimulation showed a stronger effect on the activation of prostaglandin biosynthesis than did the KLA treatment alone. Thus, the KLA/ATP double treatment produced higher levels of cyclooxygenase-2 (PGH2), and in contrast to the KLA-only treatment, the increased protein production continued even at later time points (Fig. 4*C*). The KLA/ATP stimulation also had an effect on enzymes of the 5-lipoxygenase pathway. Enzymes like microsomal glutathione *S*-transferase 3 and leukotriene A-4 hydrolase, whose abundance was significantly decreased with the KLA treatment, showed either no significant change or a slight decrease in protein abundance with the double stimulation.

Overall, this work has broad implications for understanding primary macrophage function (29). Importantly, it provides comprehensive proteomic data (30) and thus completes the full overview of the eicosanoid pathway that our group initiated some years ago (4), which now includes metabolomic, transcriptomic, and proteomic data for the same set of experimental conditions.

* This work was supported by National Institutes of Health Large Scale Collaborative LIPID MAPS Grant GM069338 (to E. A. D.), by funds from the European Research Council (to R. A.), and by the European Union via European Research Council Advanced Grant 233226 (to R. A.), and by the LiverX program of the Swiss Initiative for Systems Biology (SystemsX) (to E. S.).

[S] This article contains supplemental material.

‡‡ To whom correspondence should be addressed: Dept. of Chemistry and Biochemistry and Department of Pharmacology, School of Medicine, University of California, San Diego, La Jolla, CA 92093-0601. E-mail: edennis@ucsd.edu.

¶¶ To whom correspondence should be addressed: Institute for Molecular Systems Biology, ETH-Zürich, Wolfgang-Pauli-Strasse 16, 8093 Zürich, Switzerland. E-mail: aebersold@imsb.biol.ethz.ch.

REFERENCES

1. Khanapure, S. P., Garvey, D. S., Janero, D. R., and Letts, L. G. (2007) Eicosanoids in inflammation: Biosynthesis, pharmacology, and therapeutic frontiers. *Curr. Top. Med. Chem.* **7,** 311–340
2. Medzhitov, R. (2008) Origin and physiological roles of inflammation. *Nature* **454,** 428–435
3. Medzhitov, R. (2010) Inflammation 2010: New adventures of an old flame. *Cell* **140,** 771–776
4. Buczynski, M. W., Dumlao, D. S., and Dennis, E. A. (2009) Thematic review series: Proteomics. An integrated omics analysis of eicosanoid biology. *J. Lipid Res.* **50,** 1015–1038
5. Harkewicz, R., Fahy, E., Andreyev, A., and Dennis, E. A. (2007) Arachidonate-derived dihomoprostaglandin production observed in endotoxin-stimulated macrophage-like cells. *J. Biol. Chem.* **282,** 2899–2910
6. Buczynski, M. W., Stephens, D. L., Bowers-Gentry, R. C., Grkovich, A., Deems, R. A., and Dennis, E. A. (2007) TLR-4 and sustained calcium agonists synergistically produce eicosanoids independent of protein synthesis in RAW264.7 cells. *J. Biol. Chem.* **282,** 22834–22847
7. Raetz, C. R., Garrett, T. A., Reynolds, C. M., Shaw, W. A., Moore, J. D., Smith, D. C., Jr., Ribeiro, A. A., Murphy, R. C., Ulevitch, R. J., Fearns, C., Reichart, D., Glass, C. K., Benner, C., Subramaniam, S., Harkewicz, R., Bowers-Gentry, R. C., Buczynski, M. W., Cooper, J. A., Deems, R. A., and Dennis, E. A. (2006) Kdo2-Lipid A of *Escherichia coli*, a defined endotoxin that activates macrophages via TLR-4. *J. Lipid Res.* **47,** 1097–1111
8. Gupta, S., Maurya, M. R., Stephens, D. L., Dennis, E. A., and Subramaniam, S. (2009) An integrated model of eicosanoid metabolism and signaling based on lipidomics flux analysis. *Biophys. J.* **96,** 4542–4551
9. Dennis, E. A., Deems, R. A., Harkewicz, R., Quehenberger, O., Brown, H. A., Milne, S. B., Myers, D. S., Glass, C. K., Hardiman, G., Reichart, D., Merrill, A. H., Jr., Sullards, M. C., Wang, E., Murphy, R. C., Raetz, C. R., Garrett, T. A., Guan, Z., Ryan, A. C., Russell, D. W., McDonald, J. G., Thompson, B. M., Shaw, W. A., Sud, M., Zhao, Y., Gupta, S., Maurya, M. R., Fahy, E., and Subramaniam, S. (2010) A mouse macrophage lipidome. *J. Biol. Chem.* **285,** 39976–39985
10. Picotti, P., Rinner, O., Stallmach, R., Dautel, F., Farrah, T., Domon, B., Wenschuh, H., and Aebersold, R. (2010) High-throughput generation of selected reaction-monitoring assays for proteins and proteomes. *Nat. Methods* **7,** 43–46
11. Martens, L., Hermjakob, H., Jones, P., Adamski, M., Taylor, C., States, D., Gevaert, K., Vandekerckhove, J., and Apweiler, R. (2005) PRIDE: The proteomics identifications database. *Proteomics* **5,** 3537–3545
12. Desiere, F., Deutsch, E. W., King, N. L., Nesvizhskii, A. I., Mallick, P., Eng, J., Chen, S., Eddes, J., Loevenich, S. N., and Aebersold, R. (2006) The PeptideAtlas project. *Nucleic Acids Res.* **34,** D655–D658
13. Mallick, P., Schirle, M., Chen, S. S., Flory, M. R., Lee, H., Martin, D., Ranish, J., Raught, B., Schmitt, R., Werner, T., Kuster, B., and Aebersold, R. (2007) Computational prediction of proteotypic peptides for quantitative proteomics. *Nat. Biotechnol.* **25,** 125–131
14. Lange, V., Picotti, P., Domon, B., and Aebersold, R. (2008) Selected reaction monitoring for quantitative proteomics: A tutorial. *Mol. Syst. Biol.* **4,** 222 10.1038/msb.2008.61
15. Elias, J. E., and Gygi, S. P. (2007) Target-decoy search strategy for increased confidence in large-scale protein identifications by mass spectrometry. *Nat. Methods* **4,** 207–214
16. Picotti, P., Bodenmiller, B., Mueller, L. N., Domon, B., and Aebersold, R. (2009) Full dynamic range proteome analysis of *S. cerevisiae* by targeted proteomics. *Cell* **138,** 795–806
17. Zien, A., Aigner, T., Zimmer, R., and Lengauer, T. (2001) Centralization: A new method for the normalization of gene expression data. *Bioinformatics* **17,** (Suppl. 1), S323–S331
18. Chang, C. Y., Picotti, P., Huettenhain, R., Heinzelmann-Schwarz, V., Jovanovic, M., Aebersold, R., and Vitek, O. (2011) Protein significance analysis in selected reaction monitoring (SRM) measurements. *Mol. Cell Proteomics* 10.1074/mcp.M111.014662
19. Benjamini, Y., and Hochberg, Y. (1995) Controlling the false discovery rate: A practical and powerful approach to multiple testing. *J. R. Stat. Soc. Series B* **57,** 289–300
20. Hempel, S. L., Monick, M. M., and Hunninghake, G. W. (1994) Lipopolysaccharide induces prostaglandin H synthase-2 protein and mRNA in human alveolar macrophages and blood monocytes. *J. Clin. Invest.* **93,**

391–396
21. Lee, S. H., Soyoola, E., Chanmugam, P., Hart, S., Sun, W., Zhong, H., Liou, S., Simmons, D., and Hwang, D. (1992) Selective expression of mitogen-inducible cyclooxygenase in macrophages stimulated with lipopolysaccharide. *J. Biol. Chem.* **267,** 25934–25938
22. Dennis, E. A., Cao, J., Hsu, Y. H., Magrioti, V., and Kokotos, G. (2011) Phospholipase A2 enzymes: Physical structure, biological function, disease implication, chemical inhibition, and therapeutic intervention. *Chem. Rev.* **111,** 6130–6185
23. Rådmark, O., Werz, O., Steinhilber, D., and Samuelsson, B. (2007) 5-Lipoxygenase: Regulation of expression and enzyme activity. *Trends Biochem. Sci.* **32,** 332–341
24. Werz, O. (2002) 5-Lipoxygenase: Cellular biology and molecular pharmacology. *Curr. Drug Targets Inflamm. Allergy* **1,** 23–44
25. Peters-Golden, M., and Brock, T. G. (2003) 5-lipoxygenase and FLAP. *Prostaglandins Leukot. Essent. Fatty Acids* **69,** 99–109
26. Suzuki, K., Yamamoto, T., Sato, A., Murayama, T., Amitani, R., Yamamoto, K., and Kuze, F. (1993) Lipopolysaccharide primes human alveolar macrophages for enhanced release of superoxide anion and leukotriene B4: Self-limitations of the priming response with protein synthesis. *Am. J. Respir. Cell Mol. Biol.* **8,** 500–508
27. Aderem, A. A., Cohen, D. S., Wright, S. D., and Cohn, Z. A. (1986) Bacterial lipopolysaccharides prime macrophages for enhanced release of arachidonic acid metabolites. *J. Exp. Med.* **164,** 165–179
28. Ulmann, L., Hirbec, H., and Rassendren, F. (2010) P2X4 receptors mediate PGE2 release by tissue-resident macrophages and initiate inflammatory pain. *EMBO J.* **29,** 2290–2300
29. Norris, P. C., Reichart, D., Dumlao, D. S., Glass, C. K., and Dennis, E. A. (2011) Specificity of eicosanoid production depends on the TLR-4-stimulated macrophage phenotype. *J. Leukoc. Biol.* **90,** 563–574
30. Dennis, E. A. (2009) Lipidomics joins the omics evolution. *Proc. Natl. Acad. Sci. U.S.A.* **106,** 2089–2090